Differential cross section for n-p elastic scattering in the angular range $60° < \theta^* < 180°$ at 801.9 MeV

Mahavir Jain,* M. L. Evans,† G. Glass, J. C. Hiebert, R. A. Kenefick, and L. C. Northcliffe
Texas A&M University, College Station, Texas 77843

B. E. Bonner and J. E. Simmons
Los Alamos National Laboratory, Los Alamos, New Mexico 87545

C. W. Bjork* and P. J. Riley
University of Texas, Austin, Texas 78712

H. C. Bryant, C. G. Cassapakis,‡ B. Dieterle, C. P. Leavitt, and D. M. Wolfe
University of New Mexico, Albuquerque, New Mexico 87131

D. W. Werren§
University of Geneva, Geneva, Switzerland
(Received 17 April 1984)

The differential cross section for n-p elastic scattering at 801.9 MeV has been measured with high statistical precision and good relative accuracy over the angular range $60° < \theta^* < 180°$. The absolute normalization is based on the simultaneously observed yield of deuterons from the $np \rightarrow d\pi^0$ reaction and is good to 7%. A nearly monoenergetic neutron beam, produced by proton bombardment of a liquid-deuterium target, was directed through a liquid-hydrogen target. The angle, velocity, and momentum of charged particles ejected from the target were measured in a magnetic spectrometer equipped with multiwire proportional chambers and timing scintillators. The results are in good agreement with earlier Saclay and LAMPF data and include an angular region not covered before. The pole-extrapolation method of Chew was used to extract a value $f^2 = 0.075 \pm 0.005$ for the pion-nucleon coupling constant which is in agreement with accepted values, thus providing evidence for the accuracy of the shape and normalization of the angular distribution.

I. INTRODUCTION

In recent years, much progress has been made toward a determination of the nucleon-nucleon interaction in the energy region from 200 to 800 MeV. The quality and variety of p-p elastic scattering data are now sufficient for the establishment of unambiguous and relatively accurate $I = 1$ phase-shift solutions for the whole energy region. The accumulation of good n-p scattering data for energies up to ~ 650 MeV has led to a similar but less accurate determination of the $I = 0$ phase shifts for that region.[1] Above 650 MeV, however, the situation is less certain, because of the fewer data available, the larger number of partial waves involved, and the greater importance of inelasticity.

The N-N data which were available in 1978 are contained in a compilation by Bystricky and Lehar.[2] For energies near 800 MeV the n-p data include values for the total cross section[3,4] and several measurements of the c.m. differential cross section $d\sigma/d\Omega^*$ for various c.m. angular ranges: for $50° < \theta^* < 180°$ at 817 MeV from the Princeton-Pennsylvania Accelerator (PPA);[5] for $135° < \theta^* < 180°$ at 772 and 814 MeV from Saclay;[6] for $110° < \theta^* < 180°$ at 771 MeV from the Clinton P. Anderson Meson Physics Facility (LAMPF);[7] and for the forward angle region $10° < \theta^* < 65°$ at 790 MeV from LAMPF.[8] The PPA values are in considerable disagreement with the others. Few measurements of the analyzing power $A(\theta^*)$ or polarization $P(\theta^*)$ have been published,[9–11] but several as yet unpublished sets[12–15] have been used in a current phase-shift analysis.[16] In addition, there is a small set of polarization transfer measurements at 790 MeV,[10] and a few measurements of the Wolfenstein D and A parameters.[12] In the present paper the results of a measurement at LAMPF of $d\sigma/d\Omega^*$ for the angular range $60° < \theta^* < 180°$ at 801.9 MeV are presented.

II. EXPERIMENTAL METHOD

Since the experiment was performed using the same apparatus and techniques as in a previously reported measurement at 647.5 MeV,[17] only the briefest description will be given here. A nearly monoenergetic neutron beam was obtained by tight collimation of the 0° neutrons produced in proton bombardment of a liquid deuterium target of 10.8 cm thickness.[18] The proton beam was magnetically deflected, after passage through the target, and was stopped behind a shield wall. The neutron spectrum is shown in Fig. 1. The neutrons used in this experiment were those in the sharp charge-exchange (CE) peak at the high energy end of the spectrum. The beam passed through a liquid-hydrogen (LH_2) target of thickness 13.2

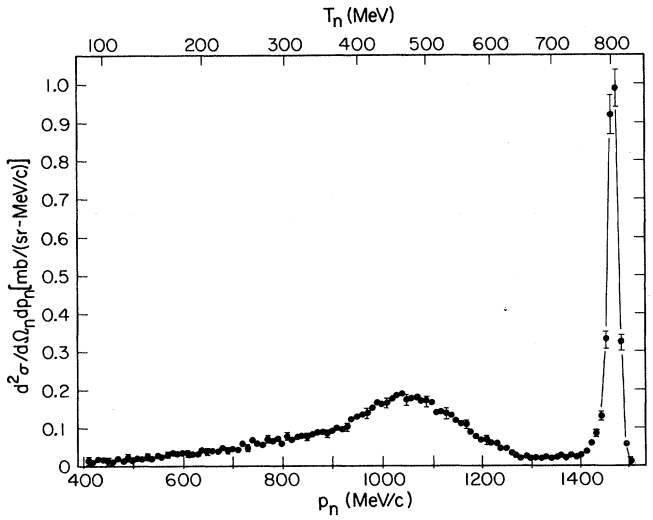

FIG. 1. Momentum spectrum of the neutron beam.

cm, and individual charged particles ejected from the target were detected in a magnetic spectrometer equipped with four multiwire proportional chambers (MWPC's), which overdetermined the particle trajectories by providing horizontal (x) and vertical (y) coordinates for the path at two locations in front of and two behind the magnet. Thin scintillator planes S_1 and S_2 located at the front and back ends of the spectrometer provided timing information. From the deflections of the particles ($\sim 22°$) and their flight times through the spectrometer, particle identification and a momentum measurement of accuracy $\sim 0.7\%$ could be made. The spectrometer could be moved on an arc centered on the target. It had an angular acceptance of $\sim 4°$, and nominal spectrometer placements at 4° increments were used in the experiment. The uncertainties in laboratory scattering angle arose from multiple scattering in the LH_2 target and scintillator S_1 ($\pm 0.08°$ at $\sim 0°$ to $\pm 0.30°$ at $\sim 55°$), from multiple scattering and geometrical resolution effects within the spectrometer ($\pm 0.07°$ at $\sim 0°$ to $\pm 0.16°$ at $\sim 55°$), and from uncertainties in the spectrometer position and the MWPC alignment ($\pm 0.10°$). Combined in quadrature these give overall uncertainties in laboratory angle ranging from $\pm 0.15°$ at $\sim 0°$ to $\pm 0.35°$ at $\sim 55°$. The corresponding errors in θ^* range from $\pm 0.36°$ at $\sim 180°$ to $\pm 0.64°$ at $\sim 60°$.

The neutron beam flux was monitored by a pair of counter telescopes placed symmetrically at 25° to the left and right of the beam axis, which viewed a polyethelene radiator disk of thickness 2.54 cm placed in the beam at the collimator exit. The calibration for this monitor was provided by measurement, in the MWPC spectrometer, of the yield of deuterons from the reaction $np \rightarrow d\pi^0$; by isospin conservation the cross section for this reaction is expected to be one-half of that for the reaction $pp \rightarrow d\pi^+$, and the latter cross section is reasonably well known ($\sim 5\%$ accuracy[19]). The overall accuracy of this method of normalization is estimated to be $\sim 7\%$.[20]

The criterion for acceptance of events was a coincidence between signals from S_1,S_2 and signals from at least three each out of the four x and four y planes. The data for acceptable events were sent to a computer which wrote them onto magnetic tape for off-line processing. At each spectrometer angle, data were taken with the LH_2 target cell both filled and emptied, so as to determine the background scattering from the target cell walls. This background was 5—10% of the total, and the fraction of time spent determining it varied from $\sim \frac{1}{5}$ where it was low to $\sim \frac{2}{3}$ where it was higher. The number of events accepted for full-target runs varied from $\sim 400\,000$ at 0° to $\sim 36\,000$ at each of the six largest angles.

In the off-line analysis, the momentum for each event was determined from the MWPC coordinate data and a map of the spectrometer magnetic field by a procedure which began with the coordinates of the incident path and an estimate of the momentum (given by the overall deflection); a numerical integration of the horizontal deflection through the spectrometer was performed so as to obtain calculated coordinates of the emergent path, which were compared with the observed coordinates. A χ^2 minimization process was then used to adjust the incident coordinates and momentum for optimum agreement between the calculated and measured coordinate information. Further details on this procedure can be found in Ref. 17.

Deuterons were distinguished from protons of the same momenta by the difference in their flight time through the spectrometer and by the difference in the pulse height they produced in S_2. Since a fraction of the flight times were corrupted by accidental coincidences, the second test was an important added constraint.

The deuterons from the $np \rightarrow d\pi^0$ reaction fall on a well-defined locus on a plot of momentum versus scattering angle. These data were analyzed separately to determine their relative angular distribution in the c.m. system, which was assumed to have the functional form

$$d\sigma/d\Omega^* = A + \cos^2\theta^* + B\cos^4\theta^* .$$

The values of A and B were determined in a least-squares fit to the data and were found to be $A = 0.317$ and $B = -0.471$.[21] In accord with isospin conservation the cross section for the $pp \rightarrow d\pi^+$ reaction is expected to be twice that for the $np \rightarrow d\pi^0$ reaction, presumably at the same deuteron c.m. momentum. The proton energy in $pp \rightarrow d\pi^+$ which corresponds to the mean neutron energy of the present experiment (801.9 MeV) is 809.1 MeV, at which the total cross section for $pp \rightarrow d\pi^+$ was taken to be $\sigma_p = 1.22$ mb. Thus the $np \rightarrow d\pi^0$ total cross section was taken to be $\sigma_n = 0.61$ mb in calibration of the neutron flux monitor.

In the analysis of the n-p elastic scattering data, the apparent incident neutron spectrum was reconstructed from the observed recoil proton spectrum through use of the known n-p kinematics. Only events which fell within a narrow window containing the $pd \rightarrow n$ quasifree CE peak of the reconstructed neutron spectrum were used in the n-p cross section determination. As the spectrometer was moved to larger angles, the CE peak of the reconstructed spectrum was broadened and shifted by plural and multiple scattering and energy-loss effects in the LH_2 target and the spectrometer, and window placement became less certain. A correction for imperfect window placement was generated with a Monte Carlo calculation, which is

TABLE I. Differential cross section for n-p elastic scattering at 801.9 MeV.

θ^* (deg)	$d\sigma/d\Omega^*$ (mb/sr)	$-u$ (GeV/c)^2	$d\sigma/du$ [mb/(GeV/c)^2]	θ^* (deg)	$d\sigma/d\Omega^*$ (mb/sr)	$-u$ (GeV/c)^2	$d\sigma/du$ [mb/(GeV/c)^2]	θ^* (deg)	$d\sigma/d\Omega^*$ (mb/sr)	$-u$ (GeV/c)^2	$d\sigma/du$ [mb/(GeV/c)^2]
179.62	8.144±0.193	0.0000	68.01±1.61	142.22	1.456±0.060	0.1576	12.16±0.50	100.00	0.456±0.030	0.6210	3.81±0.25
178.87	8.038±0.111	0.0001	67.12±0.92	141.49	1.497±0.058	0.1635	12.50±0.48	99.34	0.407±0.030	0.6295	3.40±0.25
178.12	7.900±0.085	0.0004	65.97±0.71	140.76	1.404±0.060	0.1695	11.72±0.50	98.69	0.429±0.031	0.6380	3.58±0.26
177.37	7.622±0.074	0.0008	63.65±0.62	140.03	1.260±0.058	0.1755	10.53±0.48	93.15	0.423±0.031	0.7102	3.53±0.26
176.61	7.348±0.093	0.0013	61.36±0.78	139.31	1.272±0.055	0.1817	10.62±0.46	92.50	0.452±0.030	0.7187	3.77±0.25
175.86	7.025±0.094	0.0020	58.67±0.79	138.58	1.337±0.055	0.1880	11.17±0.46	91.86	0.432±0.031	0.7271	3.61±0.26
175.11	6.729±0.149	0.0027	56.19±1.24	136.59	1.131±0.043	0.2055	9.45±0.36	91.22	0.451±0.035	0.7356	3.76±0.29
174.36	6.155±0.144	0.0036	51.40±1.20	135.87	1.135±0.045	0.2121	9.48±0.37	90.57	0.431±0.030	0.7440	3.60±0.25
173.60	5.898±0.191	0.0047	49.25±1.60	135.15	1.097±0.046	0.2187	9.16±0.38	89.93	0.447±0.033	0.7524	3.74±0.27
172.85	6.006±0.193	0.0058	50.15±1.61	134.43	1.044±0.043	0.2254	8.72±0.36	89.29	0.480±0.031	0.7608	4.00±0.26
172.10	5.043±0.113	0.0071	42.11±0.94	133.71	0.956±0.046	0.2322	7.98±0.38	88.65	0.501±0.034	0.7691	4.18±0.28
171.35	4.809±0.110	0.0085	40.16±0.92	133.00	0.930±0.041	0.2390	7.76±0.35	88.02	0.515±0.038	0.7775	4.30±0.31
170.60	4.778±0.110	0.0101	39.90±0.91	132.28	0.856±0.042	0.2459	7.15±0.35	83.29	0.503±0.034	0.8393	4.20±0.28
169.84	4.278±0.105	0.0118	35.73±0.88	131.56	0.929±0.042	0.2529	7.76±0.35	82.66	0.490±0.036	0.8474	4.09±0.30
169.09	4.368±0.105	0.0136	36.48±0.87	130.85	0.902±0.041	0.2600	7.53±0.34	82.04	0.599±0.040	0.8556	5.00±0.33
168.34	4.010±0.101	0.0155	33.49±0.85	130.14	0.921±0.042	0.2671	7.69±0.35	81.41	0.590±0.039	0.8637	4.93±0.32
167.59	4.066±0.102	0.0175	33.96±0.85	128.38	0.851±0.060	0.2849	7.11±0.50	80.79	0.593±0.039	0.8717	4.96±0.32
166.84	3.884±0.100	0.0197	32.44±0.84	127.67	0.840±0.059	0.2923	7.02±0.49	80.17	0.653±0.039	0.8798	5.46±0.33
166.09	3.713±0.126	0.0220	31.01±1.05	126.96	0.892±0.061	0.2997	7.45±0.51	79.55	0.619±0.040	0.8878	5.17±0.33
165.34	3.457±0.122	0.0244	28.87±1.02	126.25	0.684±0.054	0.3071	5.71±0.45	78.93	0.577±0.040	0.8958	4.82±0.34
164.59	3.420±0.115	0.0270	28.56±0.96	125.55	0.754±0.057	0.3146	6.29±0.48	78.31	0.648±0.040	0.9037	5.41±0.33
163.85	3.618±0.117	0.0296	30.22±0.98	124.84	0.614±0.053	0.3222	5.13±0.44	77.70	0.588±0.041	0.9116	4.91±0.34
163.10	3.346±0.092	0.0324	27.94±0.77	124.14	0.770±0.058	0.3298	6.43±0.48	77.11	0.738±0.043	0.9192	6.16±0.36
162.35	3.337±0.092	0.0353	27.87±0.76	123.43	0.673±0.054	0.3374	5.62±0.45	76.49	0.694±0.046	0.9270	5.79±0.38
161.60	3.178±0.090	0.0384	26.54±0.75	117.75	0.583±0.033	0.4016	4.87±0.27	75.88	0.646±0.042	0.9348	5.39±0.35
160.86	3.002±0.086	0.0415	25.07±0.72	117.06	0.615±0.032	0.4097	5.13±0.27	75.27	0.662±0.048	0.9426	5.53±0.40
160.11	3.092±0.088	0.0448	25.82±0.73	116.36	0.513±0.030	0.4178	4.29±0.25	74.66	0.701±0.047	0.9503	5.86±0.39
159.36	3.085±0.088	0.0482	25.76±0.73	115.67	0.535±0.034	0.4259	4.47±0.28	74.05	0.778±0.048	0.9580	6.50±0.40
158.62	2.995±0.086	0.0517	25.01±0.72	114.99	0.553±0.032	0.4341	4.62±0.27	73.44	0.816±0.052	0.9657	6.82±0.43
157.87	2.767±0.085	0.0553	23.11±0.71	114.30	0.504±0.031	0.4423	4.21±0.26	72.83	0.821±0.051	0.9733	6.86±0.42
157.13	2.387±0.129	0.0590	19.93±1.08	113.61	0.525±0.030	0.4505	4.39±0.25	72.22	0.703±0.049	0.9809	5.87±0.41
156.39	2.609±0.135	0.0629	21.78±1.13	112.93	0.561±0.031	0.4587	4.69±0.26	68.29	0.951±0.057	1.0295	7.94±0.47
155.64	2.488±0.132	0.0668	20.78±1.10	112.24	0.526±0.031	0.4670	4.40±0.26	67.69	0.934±0.054	1.0368	7.80±0.45

TABLE I (*Continued*).

θ^* (deg)	$d\sigma/d\Omega^*$ (mb/sr)	$-u$ (GeV/c)^2	$d\sigma/du$ [mb/(GeV/c)^2]	θ^* (deg)	$d\sigma/d\Omega^*$ (mb/sr)	$-u$ (GeV/c)^2	$d\sigma/du$ [mb/(GeV/c)^2]	θ^* (deg)	$d\sigma/d\Omega^*$ (mb/sr)	$-u$ (GeV/c)^2	$d\sigma/du$ [mb/(GeV/c)^2]
153.99	2.498±0.091	0.0761	20.86±0.76	111.56	0.537±0.032	0.4753	4.49±0.27	67.09	1.061±0.059	1.0440	8.86±0.49
153.25	2.408±0.092	0.0804	20.11±0.77	110.19	0.480±0.029	0.4921	4.01±0.24	66.50	1.108±0.059	1.0512	9.25±0.49
152.51	2.346±0.089	0.0849	19.59±0.74	109.51	0.484±0.030	0.5005	4.04±0.25	65.90	1.141±0.060	1.0583	9.53±0.50
151.77	2.246±0.089	0.0894	18.76±0.74	108.83	0.520±0.031	0.5089	4.34±0.26	65.31	1.137±0.067	1.0654	9.50±0.56
151.03	2.261±0.088	0.0940	18.88±0.73	108.16	0.499±0.029	0.5173	4.17±0.24	64.71	1.357±0.068	1.0725	11.33±0.57
150.29	2.220±0.086	0.0988	18.54±0.72	107.48	0.494±0.030	0.5257	4.12±0.25	64.12	1.198±0.065	1.0795	10.00±0.54
149.55	2.053±0.083	0.1036	17.14±0.69	106.81	0.497±0.030	0.5342	4.15±0.25	63.53	1.209±0.067	1.0864	10.09±0.56
148.82	2.063±0.082	0.1086	17.23±0.68	106.14	0.445±0.028	0.5426	3.71±0.24	62.94	1.347±0.067	1.0933	11.25±0.56
148.08	1.850±0.081	0.1136	15.45±0.68	105.47	0.446±0.029	0.5511	3.73±0.24	62.71	1.346±0.071	1.0960	11.24±0.59
147.35	1.840±0.079	0.1188	15.37±0.66	104.80	0.499±0.030	0.5596	4.16±0.25	62.12	1.364±0.070	1.1029	11.39±0.59
145.14	1.700±0.062	0.1349	14.20±0.51	102.65	0.414±0.030	0.5869	3.46±0.25	61.54	1.380±0.074	1.1096	11.53±0.62
144.41	1.642±0.061	0.1404	13.71±0.51	101.99	0.376±0.030	0.5954	3.14±0.25	60.95	1.510±0.076	1.1164	12.61±0.63
143.68	1.597±0.059	0.1460	13.34±0.49	101.33	0.427±0.030	0.6039	3.57±0.25	60.37	1.480±0.076	1.1231	12.36±0.63
142.95	1.609±0.061	0.1518	13.43±0.51	100.66	0.442±0.032	0.6124	3.69±0.26	59.78	1.511±0.078	1.1297	12.62±0.65

described in Ref. 17. The corrections were small at small spectrometer angle settings, but became as large as 7% at one of the larger angles. The fractional accuracy of the corrections is estimated to be 10%. Small corrections were also made for absorption of both deuterons and protons in the target and spectrometer. The corrections for protons ranged from 1% at the highest energy to zero at 300 MeV. For deuterons they were $\sim 1.7\%$.

III. RESULTS AND DISCUSSION

The center of mass differential cross section values obtained are presented in Table I, in the form $d\sigma/d\Omega^*$ as well as in the alternative form $d\sigma/du$ (where $-u$ is the square of the four-momentum transfer to the recoil proton), along with the corresponding center of mass angles θ^*. The errors quoted are statistical only. Most of the errors discussed in the preceding section were smaller (and their uncertainties much smaller) than these statistical errors. The uncertainty in the 1.7% deuteron absorption correction contributes negligibly to the normalization uncertainty of 7% assigned to the entire angular distribution. This normalization is based on the assumption that the total cross section $\sigma_n(801.9)$ for the $np \rightarrow d\pi^0$ reaction at 801.9 MeV is 0.61 mb. If a future determination leads to a different and better value of $\sigma_n(801.9)$, the cross section values of Table I should be renormalized through multiplication by the factor $\sigma_n(801.9)/0.61$ mb. As noted earlier, the uncertainties in θ^* range from $\pm 0.36°$ at 180° to $\pm 0.64°$ at 60°, which correspond to uncertainties in $d\sigma/d\Omega^*$ of 0.6% and 3.2%, respectively.

A. Comparison with other experiments

The results of the present experiment are compared with the 817 MeV data from PPA (Ref. 5) and the forward angle 790 MeV data of Carlini *et al.*[8] in Fig. 2. The agreement between the results of the present experiment and those of Ref. 8 is good, but there is strong disagreement with the data of Ref. 5. In Fig. 3 the present results are compared with the 814 MeV results from Saclay[6] in the back-angle CE region. The agreement is excellent from 134° to 164°, but for larger angles the Saclay values tend to be higher. The Saclay measurements at 772 MeV (Ref. 6) and the LAMPF measurements at 771 MeV (Ref. 7) are not shown in Fig. 3. Both sets span the CE region, 135°–180° for Ref. 6 and 110°–180° for Ref. 7. Both give values of $d\sigma/d\Omega^*$ slightly higher than those of this experiment, and diverge somewhat at the larger angles. The differences are far less, however, than the disagreement with Ref. 5.

B. Phase shift fit

Also shown in Fig. 2 is the differential cross section curve predicted by a phase-shift fit labeled C800. This fit was obtained with the computer program of Arndt *et al.*[1] making use of an extended set of both published and unpublished p-p, n-p, and p-n (quasifree) data in the

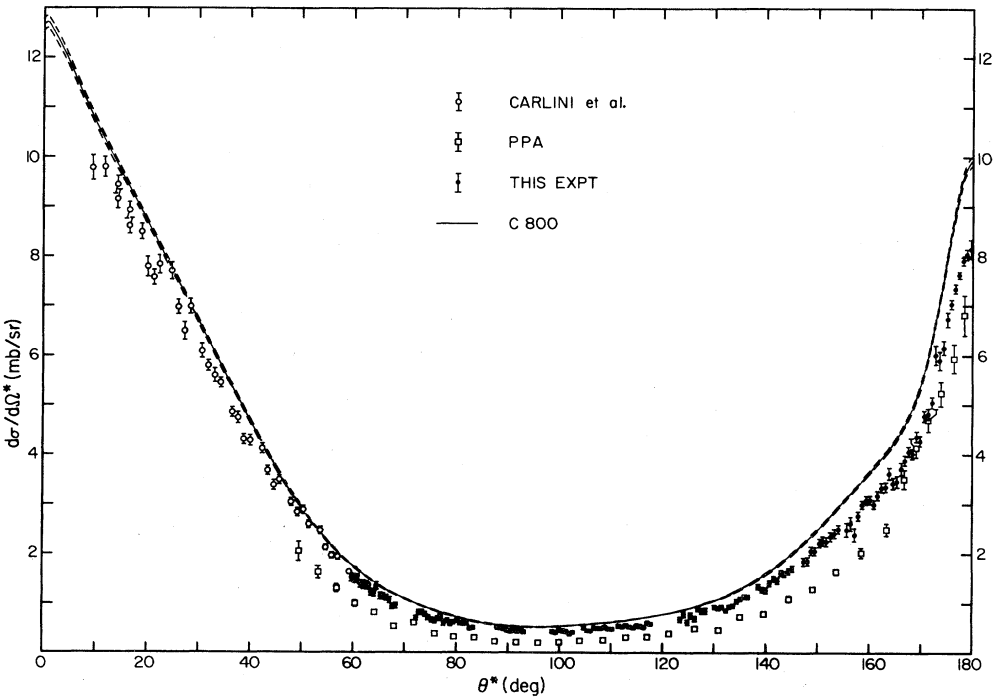

FIG. 2. Comparison of n-p differential cross section measurements near 800 MeV. The results of the present experiment (●) are compared with the results of Carlini *et al.* (○) (Ref. 8), with the PPA results (□) (Ref. 5), and with the prediction of a phase-shift fit, C800, obtained with the code of Arndt *et al.* (Ref. 16).

765—835 MeV energy region. The n-p data base included the differential cross section data of this experiment and the two other LAMPF experiments[7,8] and the data from Saclay,[6] but not those from PPA.[5] In addition, it contained total cross section data,[3,4] n-p and p-n polarization and analyzing power data,[9–15] and some polarization transfer[10] and Wolfenstein D and A parameter data.[12]

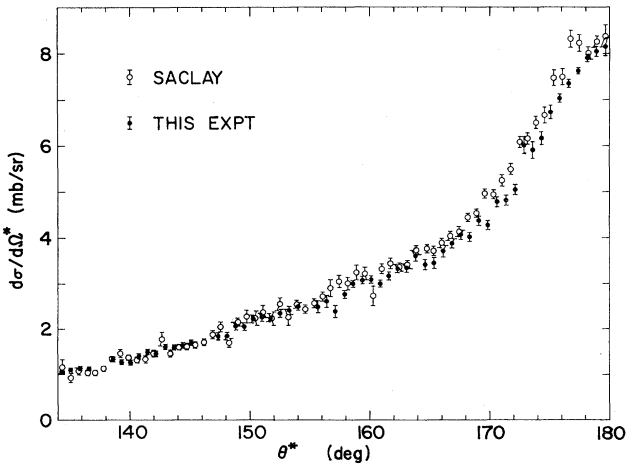

FIG. 3. Comparison of n-p cross sections in the charge-exchange region obtained in this experiment (●) with the Saclay data at 814.3 MeV (○) (Ref. 6).

The fit was made with 34 free parameters, including coupling parameters up to ϵ_6 and partial-wave phase shifts up to ${}^3J_6$. The $I=1$ parameters were determined primarily by the p-p data and the $I=0$ parameters by the n-p data. The n-p data set included 398 points and the χ^2 value for the fit to the renormalized points (see below) was 732, giving χ^2 per degree of freedom $(\chi^2_\nu)=2.0$. The error corridors indicated by the dashed lines in Fig. 2 show the range of predictions given by fits for which the value of χ^2 per datum is increased by 1.0 above its minimum value.

It is common practice to float the normalization of data from individual experiments in the phase-shift fitting process. The renormalization factor obtained for the present data in the C800 fit was 1.20, well beyond the 7% normalization uncertainty assigned to these data because of uncertainties in the $pp\rightarrow d\pi^+$ cross section and possible isospin noninvariance. The reason for this discrepancy is not understood, but the good agreement of the present data with those of Carlini *et al.*[8] at angles near 60° common to both data sets is evidence for the correctness of the present normalization; the normalization method was entirely different in the two experiments. An additional reason for believing the present normalization will be given in the next section.

C. Charge exchange region

The shape of the peak in the backward angle (CE) region is not well understood, but must be influenced by

TABLE II. Two-exponential fits to the n-p charge-exchange scattering data in the 800 MeV energy region. The angular range is approximately $135° < \theta^* < 180°$.

Expt.	Ref.	T (MeV)	No. of points	α_1	β_1	α_2	β_2	χ^2_ν
PPA	5	817	13	20.4±1.5	5.86±0.55	32.3±2.0	61±8	0.84
Saclay	6	814.3	65	34.8±0.5	6.91±0.13	34.0±0.6	128±5	1.43
Present		801.9	59	33.4±0.4	6.16±0.09	34.4±0.5	149±6	1.12

one-pion exchange effects. It has long been known,[22] however, that this shape can be described rather well by the empirical double-exponential formula:

$$\frac{d\sigma}{d\Omega}=\alpha_1 e^{\beta_1 u}+\alpha_2 e^{\beta_2 u} .$$

Comparison of the values of α_1, β_1, α_2, and β_2 obtained by least-squares fitting to this formula is a convenient way of comparing the backward angle data of the various experiments. The results of such fitting for data in the CE region are presented in Table II, along with the values of χ^2_ν which measure the goodness of each fit. The agreement between the parameters for the present data and the Saclay data is fairly good, and such differences as there are may be due to the energy difference. As expected, some of the parameters are quite different for the PPA data. The fit to the data of this experiment is shown in Fig. 4.

A more meaningful and sophisticated way of determining the plausibility of the angular distribution in the CE region is to use the pole-extrapolation method of Chew[23] to extract the pion-nucleon coupling constant from the data. The method should give a value which is reasonably accurate in this energy region.[24] It is based on the conjecture that there are poles in the real part of the nucleon-nucleon scattering amplitude due to single-pion exchange at the unphysical values

$$\cos\theta^*=\pm(1+\mu^2/2k^2) ,$$

where μ is the pion rest mass and k is the nucleon c.m. momentum, as well as branch points at

$$\cos\theta^*=\pm(1+4\mu^2/2k^2),\pm(1+9\mu^2/2k^2),\ldots$$

due to higher order processes. For n-p CE scattering the $(-)$ signs are applicable and μ is the mass of the charged pion. Since our application of the method was discussed in Ref. 17, it will only be summarized here. In terms of the pion-nucleon coupling constant $g^2=(2m/\mu)^2 f^2$ (where m is the neutron rest mass), the total energy $E^*=\sqrt{k^2+m^2}$ of the neutron in the c.m. system, and the quantity $x=\cos\theta^*+1+\mu^2/2k^2$, the differential cross section can be written as[24]

$$\frac{d\sigma}{d\Omega^*}=\frac{g^2}{4E^{*2}}\frac{(1+\cos\theta^*)^2}{x^2}+\frac{A}{x}+B ,$$

where the terms containing A and B represent higher-order processes while the remainder is the one-pion contribution. Although A and B are unknown functions of x, they are known to be finite at $x=0$. The experimental values of x and $d\sigma/d\Omega^*$ are used to determine values of a new variable $y(x)$,

$$x^2\frac{d\sigma}{d\Omega^*}=y(x)=\frac{g^2}{4E^{*2}}\left[x-\frac{\mu^2}{2k^2}\right]^2+Ax+Bx^2 ,$$

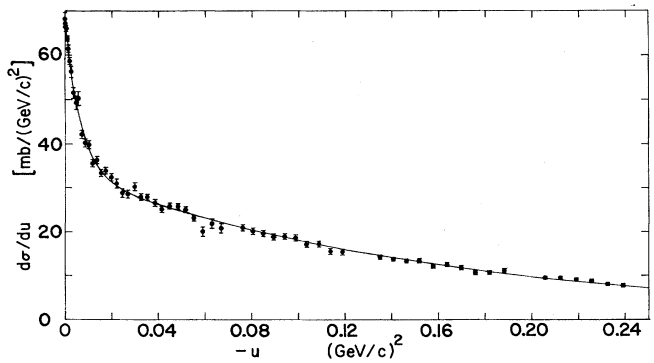

FIG. 4. Double-exponential fit to the charge-exchange scattering data ($135° < \theta^* < 180°$) of this experiment.

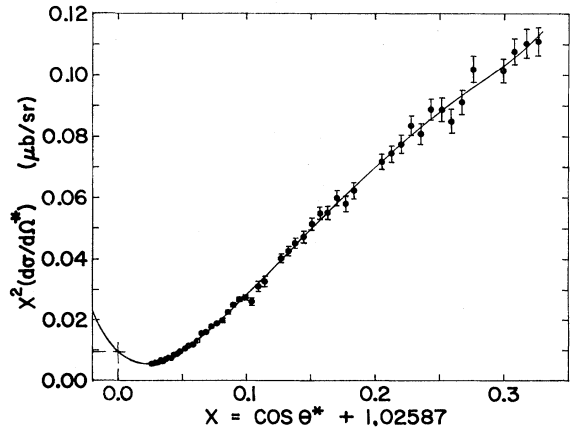

FIG. 5. Seven term polynomial fit to the values of $x^2\, d\sigma/d\Omega^*$ calculated from the data of this experiment for angles $\theta^* > 135°$.

TABLE III. Pion-nucleon coupling constant determination from this experiment.

	$135° < \theta^* < 180°$ (57 points)			$115° < \theta^* < 180°$ (76 points)			$100° < \theta^* < 180°$ (95 points)		
n	χ_ν^2	$P(n)$	f^2	χ_ν^2	$P(n)$	f^2	χ_ν^2	$P(n)$	f^2
2	28.47		imaginary	22.66		imaginary	19.28		imaginary
3	10.82	1.00	0.0132±0.0026	14.94	1.00	imaginary	13.83	1.00	imaginary
4	2.483	1.00	0.0487±0.0013	7.001	1.00	0.0270±0.0015	8.556	1.00	0.0099±0.0035
5	1.117	1.00	0.0632±0.0018	2.161	1.00	0.0515±0.0013	4.054	1.00	0.0383±0.0013
6	1.014	0.98	0.0697±0.0029	1.214	1.00	0.0631±0.0016	1.553	1.00	0.0559±0.0013
7	→1.011	0.71	0.0744±0.0051	1.145	0.97	0.0675±0.0023	1.153	1.00	0.0634±0.0016
8	1.023	0.48	0.0795±0.0088	1.147	0.66	0.0701±0.0033	1.101	0.97	0.0674±0.0022
9	1.043	0.18	0.0765±0.0157	→1.136	0.79	0.0755±0.0049	1.064	0.95	0.0719±0.0030
10	1.058	0.43	0.0608±0.0362	1.148	0.43	0.0794±0.0078	1.070	0.54	0.0695±0.0044
11							→1.030	0.96	0.0790±0.0058

which has the property that the terms containing the unknown functions A and B vanish at $x=0$. Since $x=0$ is in the unphysical region, $y(0)$ is determined by making a least-squares fit of the n-term polynomial $\sum_{i=0}^{n-1} a_i x^i$ to the physical $y(x)$ values, thus determining a_0 which is equal to $y(0)$. With some substitutions and rearrangement it follows that

$$f^2=\sqrt{a_0(k^2+m^2)}(k/m)^2 .$$

Polynomial fits in which n was varied from 2 to ~10 were made to the data for three angular regions. Two criteria were used to determine the optimum number of terms for each data set: (1) that the value of χ_ν^2 be a minimum; (2) determination by means of the F test[25] of whether the inclusion of another term significantly improved the fit, i.e., the probability $P(n)$ that χ_ν^2 was reduced significantly by the addition of the nth term was calculated. As n increases, $P(n)$ should stay near 1.0 as long as the added terms are improving the fit, but should drop sharply when the nth term does not improve the fit. Ideally, the same number of terms should be indicated by both criteria.

The results of the fitting process for increasing numbers of terms are summarized in Table III. For each data set, the fit with the optimum number of terms based on the two criteria given above is indicated by an arrow, although it could be argued that the nine-term fit is preferable to the eleven-term fit for the largest data set because the calculated error for f^2 is smaller. The fit to the angular region 135°—180° is shown in Fig. 5. The indicated fits (as well as the nine-term fit for the most extended data set) all give values of f^2 which are in agreement with a recent determination that $f^2=0.0769\pm0.0020$ obtained from an analysis of pion-nucleon scattering[26] and a determination that $f^2=0.0762\pm0.0043$ obtained from a phase-shift analysis of p-p scattering data.[27] The fact that the f^2 values deduced from these data agree with the accepted value within about 5% is evidence not only that the shape of the angular distribution is good, but also that the normalization is good.

For purposes of comparison, the polynomial fitting process was also carried out for the 817 MeV PPA and 814 MeV Saclay data for the angular range $135° < \theta^* < 180°$. The results are presented in Table IV and should be compared with the results for the same angular range in Table III. The behavior of both χ_ν^2 and $P(n)$ is erratic for the PPA data and none of the f^2 values obtained are close to the accepted value. For the Saclay data the best f^2 value, given by the six-term fit, is 22% below the accepted value. Deletion of the values for the six largest angles of the Saclay data improves the f^2 value, but it still is 9% below the accepted value.

TABLE IV. Pion-nucleon coupling constant determinations for the PPA and Saclay data for $\theta^* > 135°$.

	PPA 817 MeV (13 points)			Saclay 814 MeV (65 points)			Saclay 814 MeV (59 points)[a]		
n	χ_ν^2	$P(n)$	f^2	χ_ν^2	$P(n)$	f^2	χ_ν^2	$P(n)$	f^2
2	1.898		imaginary	15.77		imaginary	10.26		imaginary
3	1.170	0.98	imaginary	6.492	1.00	0.0029±0.0144	5.409	1.00	imaginary
4	0.852	0.94	0.0192±0.0110	1.858	1.00	0.0461±0.0016	1.797	1.00	0.0430±0.0027
5	0.931	0.36	0.0257±0.0146	1.487	1.00	0.0570±0.0024	1.385	1.00	0.0606±0.0036
6	0.818	0.81	imaginary	1.502	0.47	0.0597±0.0041	1.351	0.87	0.0698±0.0058
7	0.953	0.06	imaginary	1.474	0.85	0.0485±0.0087	1.368	0.44	0.0637±0.0113
8	1.110	0.29	imaginary	1.450	0.83	0.0130±0.0591	1.378	0.57	0.0448±0.0294
9	0.619	0.91	0.1199±0.0448	1.471	0.33	0.0369±0.0378	1.366	0.77	0.0899±0.0281
10	0.060	0.99	0.2272±0.0590	1.349	0.98	imaginary	1.294	0.94	imaginary

[a]Points for six largest angles omitted.

IV. CONCLUSIONS

The n-p differential cross section is well determined for the full angular range at 800 MeV. There is excellent agreement where the present data join the forward angle data of Carlini *et al.*[8] In the CE region there is reasonably good agreement between the present data and those of Bizard *et al.*[6] and Bonner *et al.*[7] at nearby energies. Over the entire angular range $60° < \theta^* < 180°$ there is good agreement between the data and the phase-shift prediction as to the shape of the angular distribution, but disagreement as to the normalization. The fact that the value extracted for the pion-nucleon coupling constant is in good agreement with accepted values is evidence that both the shape and normalization of the angular distribution are correct and implies that the renormalization determined in the phase-shift fit is questionable.

ACKNOWLEDGMENTS

We would like to thank J. G. J. Boissevain, D. Brown, and S. Cohen for their help in the development of the MWPC spectrometer system and electronics; J. H. Fretwell and K. D. Williamson for their help in the development and operation of the liquid-deuterium neutron production target; A. C. Niethammer for her contribution to the development of the data acquisition code; and the LAMPF staff for numerous forms of assistance during the course of the experiment. This work was supported by the U. S. Energy Research and Development Administration and the U. S. Department of Energy.

---

*Present address: Los Alamos National Laboratory, Los Alamos, NM 87545.

†Present address: Schlumberger Well Services, P.O. Box 2175, Houston, TX 78228.

‡Present address: Science Applications, Inc., LaJolla, CA 92037.

§Present address: c/o Landis X Gyr-3574, 6301 Zug, Switzerland.

[1]R. A. Arndt, L. D. Roper, R. A. Bryan, R. B. Clark, B. J. VerWest, and P. Signell, Phys. Rev. D **28**, 97 (1983).

[2]J. Bystricky and F. Lehar, Physics Data, No. 11-1 part II, N-N Data, Fachinformtionszentrum, Karlsruhe, 1978.

[3]T. J. Devlin, W. Johnson, J. Norem, K. Vosburgh, R. E. Mischke, and W. Schimmerling, Phys. Rev. D **8**, 136 (1973).

[4]P. W. Lisowski, R. E. Shamu, G. F. Auchampaugh, N. S. P. King, M. S. Moore, G. L. Morgan, and T. S. Singleton, Phys. Rev. Lett. **49**, 255 (1982).

[5]P. F. Shepard, T. J. Devlin, R. E. Mischke, and J. Solomon, Phys. Rev. D **10**, 2735 (1974).

[6]G. Bizard, F. Bonthonneau, J. L. Laville, F. LeFebvres, J. C. Malherbe, and R. Regimbart, Nucl. Phys. **B85**, 14 (1975). After publication these data were renormalized (G. Bizard, private communication). The values as tabulated in Ref. 2 have been further renormalized.

[7]B. E. Bonner, J. E. Simmons, C. L. Hollas, C. R. Newsom, P. J. Riley, G. Glass, and M. Jain, Phys. Rev. Lett. **41**, 1200 (1978).

[8]R. Carlini *et al.*, Phys. Rev. Lett. **41**, 1341 (1978).

[9]P. R. Robrish *et al.*, Phys. Lett. **31B**, 617 (1970).

[10]R. D. Ransome *et al.*, Phys. Rev. Lett. **48**, 781 (1982).

[11]T. S. Bhatia *et al.*, Phys. Rev. Lett. **48**, 227 (1982).

[12]M. L. Barlett, private communication to R. A. Arndt.

[13]C. R. Newsom *et al.*, in *Polarization Phenomena in Nuclear Physics—1980 (Fifth International Symposium, Santa Fe),* Proceedings of the Fifth International Symposium on Polarization in Nuclear Physics, AIP Conf. Proc. No. 69, edited by G. G. Ohlson, R. E. Brown, N. Jarmie, M. W. McNaughton, and G. M. Hale (AIP, New York, 1981), p. 126; private communication to R. A. Arndt by C. R. Newsom.

[14]C. L. Hollas *et al.*, in *Polarization Phenomena in Nuclear Physics—1980 (Fifth International Symposium, Santa Fe),* Proceedings of the Fifth International Symposium on Polarization Phenomena in Nuclear Physics, AIP Conf. Proc. No. 69, edited by G. G. Ohlson, R. E. Brown, N. Jarmie, M. W. McNaughton, and G. M. Hale (AIP, New York, 1981), p. 129; R. D. Ransome, private communication to R. A. Arndt.

[15]G. W. Hoffmann, private communication to R. A. Arndt.

[16]A version of the code of Ref. 1, updated September, 1983.

[17]M. L. Evans *et al.*, Phys. Rev. C **26**, 2525 (1982).

[18]C. W. Bjork *et al.*, Phys. Lett. **63B**, 31 (1976).

[19]C. Richard-Serre, W. Hirt, D. F. Measday, E. G. Michaelis, M. J. M. Saltmarsh, and P. Skarek, Nucl. Phys. **B20**, 413 (1970).

[20]D. F. Measday, private communication.

[21]M. Jain, M. L. Evans, and L. C. Northcliffe, Nucl. Phys. **A336**, 325 (1979).

[22]J. L. Friedes, H. Palevsky, R. L. Stearns, and R. J. Sutter, Phys. Rev. Lett. **15**, 38 (1965).

[23]G. F. Chew, Phys. Rev. **112**, 1380 (1958).

[24]P. Cziffra and M. J. Moravcsik, Phys. Rev. **116**, 226 (1959).

[25]P. R. Bevington, *Data Reduction and Error Analysis for the Physical Sciences* (McGraw-Hill, New York, 1969), Chap. X.

[26]V. K. Samaranayake, J. Phys. G **5**, 657 (1979).

[27]M. H. MacGregor, R. A. Arndt, and R. M. Wright, Phys. Rev. **169**, 1128 (1968).